Silyl Anions or Silylenoids?—A DFT Study of Silyllithium Compounds with π-Donating Substituents

Michaela Flock* and Christoph Marschner[a]

Abstract: Geometry optimizations at the B3LYP/6-31+G(d) level for a set of $X(SiH_3)MeSiLi$ molecules (X = F, OH, NH_2, Cl, SH, and PH_2) show that the tetrahedral structure prevails in polar solutions; however, it readily isomerizes into a silylenoid with energy barriers of less than 15 kJ mol^{-1}. Inverted structures, which predominate in the gas phase, could not be located in solution. Configuration inversion is unfavorable, with energy barriers between 80 and 220 kJ mol^{-1}. The α elimination into a silylene moiety and the corresponding LiX is only likely to occur in solution, particularly for X = Cl and SH.

Keywords: anions · density functional calculations · silicon · solvent effects · substituent effects

Introduction

In the quest for highly defined polysilanes, one of the targets is to find silyl anionic intermediates that are configurationally stable. While voluminous substituents are important factors for kinetic stability, the electronegativity and π-electron donating capabilities of the α substituents govern the configurational stability.[1] Experiments on silyl anions in the liquid phase show that some of the heteroatom-substituted molecules exist as an equilibrium between silyl anions, silylenoids (i.e., carbenoid analogues with ambiphilic behavior), and silylenes.[2] Whether the silyl anion or the silylenoid is preferred depends, among other factors, on the strength of the Si–X bond in these molecules.

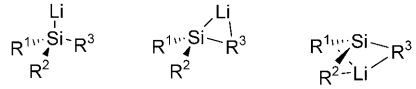

A number of compounds with silicon heteroatom bonds have been studied by theoretical and experimental means. Ab initio calculations at the Hartree–Fock and MP2 level for H_2XSiM (X = F, Cl, OMe, and M = Li, Na) find the silylenoidal and inverted structures to be the most stable.[3–6] Density functional calculations at the B3LYP/6-311++G(3df,pd) level of theory indicate that an increasing number of halogen atoms X in $X_nH_{3-n}SiM$ (M = Li and Na, n = 0–3) molecules enhances the stability of the inverted structure.[7,8] In solution, halosilyl anions form quite reactive monomers.[2] Depending on the halogen (and the substituent pattern), selfcondensation reactions,[9] complex product mixtures,[9] or typical silylene-trapping reactions are found.[10–12] Selfcondensation was also observed in the case of alkoxysilyllithium compounds,[6,13,14] but no silylene-trapping reactions. Ab initio calculations at the Hartree–Fock level indicate that the selfcondensation reaction is an exothermic process.[6] In this reaction, the nucleophilic part retains its absolute configuration while the electrophilic part undergoes an inversion. The silylenoidal character is diminished if a separated ion pair is produced, for instance, by adding crown ethers.[13,14] The best-studied species are aminosilyl anions.[15–18] Depending on the substituents, they are quite stable monomers in solution and in the solid state. Recently, Kawachi et al.[19] reported syntheses and ab initio calculations of sulfur-substituted silyllithium compounds, which were characterized as α-eliminative silylenoids. The addition of crown ethers produces separated ion pairs and thereby enhances the stability. In contrast to the heteroatom-substituted silyl anions mentioned above, nothing has yet been reported on phosphinosilyl anions to the best of our knowl-

[a] Dr. M. Flock, Prof. Dr. C. Marschner
Institute of Inorganic Chemistry
Graz University of Technology
Stremayrgasse 16, 8010 Graz (Austria)
Fax: (+43) 316-873-8701
E-mail: michaela.flock@tugraz.at

Supporting information for this article is available on the WWW under http://www.chemeurj.org/ or from the author. It contains information about the Cartesian coordinates of $X(H_3Si)MeSi^-$ and minimum structures of $X(H_3Si)MeSiLi$, $F(H_3Si)MeSiLi$ dimers, and $X(H_3Si)MeSiLi{\cdot}3\,OMe_2$.

 DOI: 10.1002/chem.200401353 © 2005 Wiley-VCH Verlag GmbH & Co. KGaA, Weinheim

edge. Recently, we were able to show that alkyl substituents increase the configurational stability of silyl anions, whereas silyl and aryl groups decrease the inversion barrier.[20]

In the present paper, we will explore the effect of α substituents with σ-electron withdrawing and π-electron donating abilities (X = F, OH, NH_2, Cl, SH, and PH_2) on the configuration stability of the chiral silyl anions X(H_3Si)MeSiLi. We will report their structures and stabilities and explore their tendency to form silylenoid structures or to dissociate into silylenes. The monomolecular inversion reactions will be investigated. The influence of solvent molecules on structures and stabilities will also be studied and compared to the respective data obtained for the gas phase and experimental results where available.

Computational Details

All geometries have been optimized at the density functional level of theory with the hybrid B3LYP functional and 6-31+G(d) basis sets as implemented in the Gaussian 98[21] program suite. The stationary points have been characterized by analytical frequency calculations. Minima have only real frequencies while transition structures have exactly one imaginary frequency. All relative energies are given in kJ mol^{-1} and have been corrected with the unscaled zero-point vibration energies. The bond angle sum, $\Sigma\alpha$, has been obtained by summing the Si–Si–C, Si–Si–X, and C–Si–X bond angles.

^{29}Si magnetic shieldings, σ^{29}Si, have been calculated by sum-over-states density functional perturbation theory (SOS-DFPT)[22] with the Perdew–Wang 91[23] functional and a 64 point radial grid by means of the deMon[24] program. IGLO B2 basis sets[25] were employed together with the following auxiliary basis functions: 5,4 for Si, P, S, and Cl; 5,2 for C, N, O, and F; 5,1 for H. Tetramethylsilane, with $\sigma_{calcd}{}^{29}$Si = 366.1 ppm, was used as the reference molecule for calculating the chemical shifts, δ^{29}Si. For comparison, we also calculated the chemical shifts at the GIAO MP2/6-311+G(d)//B3LYP/6-31+G(d) level with a magnetic shielding σ^{29}Si of 376.4 ppm for TMS.

Results and Discussion

As the starting point of this study, we describe the silyl anions. The question of silyl anion or silylenoid structures only arises when a counterion, such as lithium, is attached to the silyl anion moiety. The resulting minimum structures and their relative energies will provide information regarding the presence and stability of silylenoid structures in the gas phase. Finally, because synthetic work involving silyl anions is usually carried out in polar, mostly ethereal solutions, we add three dimethyl ether (DME) molecules to model the effect of the solvent on structures and stabilities.

Bare anions: As illustrated in Figure 1, the Si–X bond lengths of the bare anions XMe(H_3Si)Si$^-$ decrease with increasing Allred–Rochow electronegativity[26] of X: P (2.06) < S (2.44) < Cl (2.81) < N (3.07) < O (3.50) < F (4.10). This reflects the σ-acceptor strength of X. It should be noted that in other scales, such as Pauling's, for example, the electronegativity of chlorine is higher than that of nitrogen. The lone pair on X plays only a minor role. The natural bond orbital, NBO, analyses show the inductive effect of the substituent X to be a far more important factor in these cases. It was stated in the literature[1] that substituents donating electrons by resonance (π donors) or withdrawing them by induction (σ acceptors) raise the inversion barrier. This effect was explained by the destabilizing, repulsive forces between the lone pairs on Si and X being in close vicinity in the planar transition structures. NBO analyses show that the lone pair on Si is located in an sp^3-type orbital in the minimum structures. As the molecules become planar, rehybridization of this orbital occurs from sp^3 to a p orbital. For X = NH_2 and PH_2, the X lone pair in the transition structure is perpendicular to the p orbital on Si so that there is no direct interaction. Another possible explanation is that the stronger the inductive effect, the more compact is the doubly occupied p orbital on Si in the transition structure

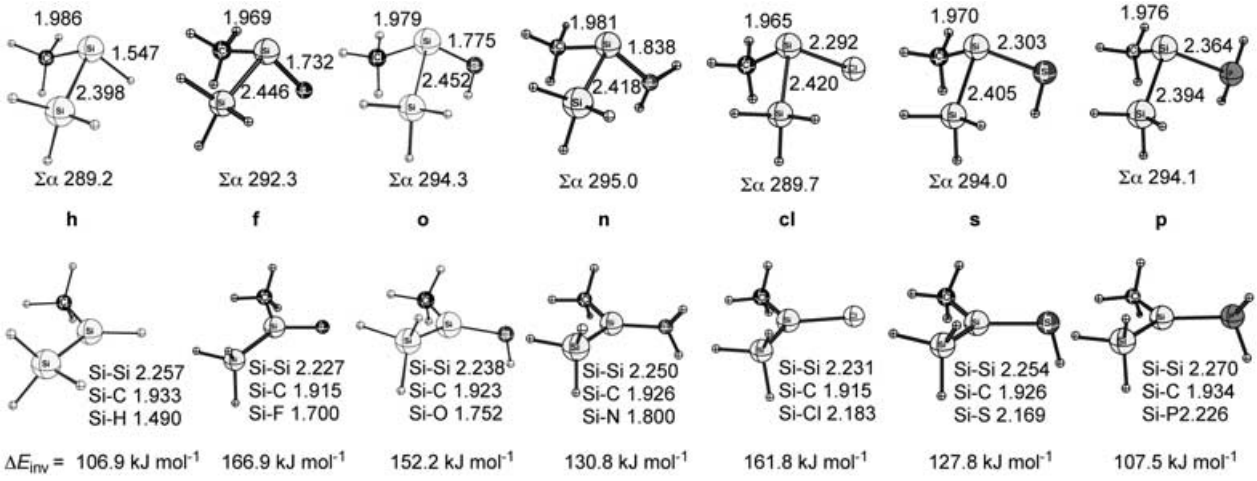

Figure 1. Geometries of the minima and transition structures of the X(H_3Si)MeSi anions with X = F, OH, NH_2, Cl, SH, and PH_2. The parent molecule H(H_3Si)MeSi$^-$ is given for reference.

© 2005 Wiley-VCH Verlag GmbH & Co. KGaA, Weinheim

making the rehybridization more difficult. In the transition structures of our molecules, both the length of the Si–Si bond and the NBO analyses indicate the formation of a dative π bond between the lone pair on the anionic Si and the SiH_3 group. This happens in the presence of at least one silyl substituent on the silyl anion. As previously seen,[20] silyl substituents decrease the inversion barrier, whereas alkyl substituents act contrarily. Compared to $Me(H_3Si)FSi^-$ ($\Delta E_{inv} = 166.9\ kJ\,mol^{-1}$), the barrier of $(H_3Si)_2FSi^-$ decreases to $120.7\ kJ\,mol^{-1}$, while for Me_2FSi^-, where the transition structure is destabilized because formation of a dative π bond does not occur, the inversion barrier increases to $267.2\ kJ\,mol^{-1}$. Within a specific substituent pattern, the inversion barriers increase with increasing electronegativity of X, which is also corroborated by our results (Figure 1). The previously reported barriers[20] for $X = SiH_3$ ($88\ kJ\,mol^{-1}$) and Me ($122.1\ kJ\,mol^{-1}$) also fit nicely into this scheme.

The more electronegative the substituent X is, the more deshielded becomes the central silicon (Table 1). The ^{29}Si chemical shifts range from $\delta = 66.9$ (X = F) to −81.7 (X = PH_2). A good correlation (correlation coefficient $c = 0.98$) between the chemical shift and the inversion energy is found for this subset. As previously reported [20] for a similar set of molecules, the deviation of IGLO/DFT relative to GIAO/MP2 calculated shieldings is systematically $\approx 20 \pm 10$ ppm (Table 1) for the bare anions. The more electronegative X, the stronger is the deviation.

Table 1. Natural charges, lone pair (LP) occupation, and ^{29}Si chemical shifts at the IGLO-DFT level (TMS, $\sigma = 366.1$ ppm) and the GIAO-MP2 level (TMS, $\sigma = 376.4$ ppm) of the $X(SiH_3)MeSi^-$ anions.

	qSi	LP_{Si}	δ^{29}Si (DFT)	δ^{29}Si (MP2)
f	0.60	1.94	66.9	96.7
o	0.57	1.92	29.1	50.9
n	0.46	1.92	−13.7	6.1
cl	0.31	1.95	44.6	73.6
s	0.20	1.92	−31.7	−12.5
p	0.05	1.91	−81.7	−68.0

Addition of Li^+: A counterion, such as Li^+, is able to attach itself to the silyl anion in different positions to yield a number of low-energy structures (Figure 2).

Characteristic bond lengths of these minima are listed in Tables 2 and 3. Compared to the bare anions, all silicon single bonds of conformer **1** are slightly contracted. This effect has been described before in a comparison of silyl anions with the respective silanes.[1,27,28] In the few crystal structures of mixed silyl- and alkyl/aryl-substituted lithiosilanes forming dimers in apolar solvents,[29–32] bond lengths of approximately 2.34 Å and 1.94 Å were measured for Si–Si and Si–C bonds. The Si–Li dimer

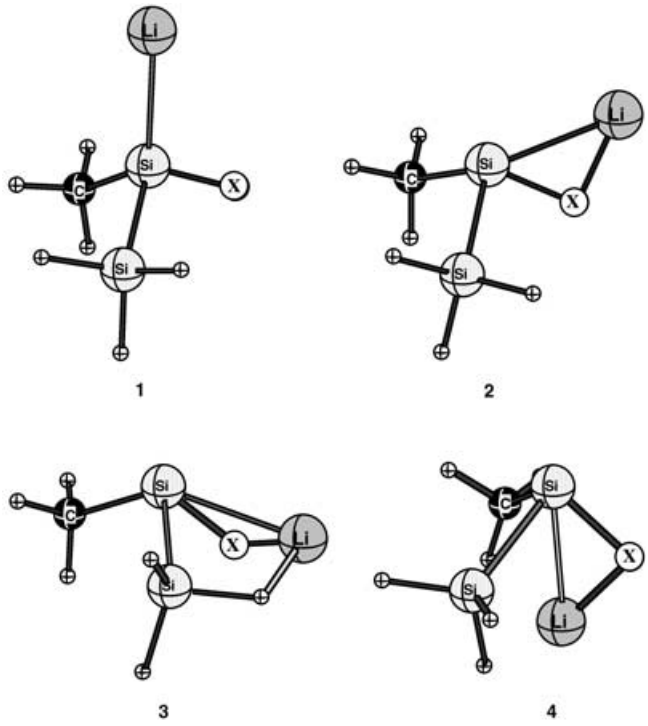

Figure 2. Tetrahedral **1**, silylenoid (**2** and **3**), and inverted (**4**) structures of $X(H_3Si)MeSiLi$ (X = F, Cl, OH, SH, NH_2, PH_2) in the gas phase. Molecule code: carbon = solid black, silicon = dotted, and lithium = striped.

Table 2. Selected bond lengths (Å), δ^{29}Si, Si–X stretching frequency, and ZPVE-corrected relative energies ($kJ\,mol^{-1}$) for the tetrahedral and inverted structures **1** and **4** of the $X(SiH_3)MeSiLi$ molecules.

	1h	**1f**	**1o**	**1n**	**1cl**	**1s**	**1p**
Si–X	1.511	1.686	1.703	1.789	–	2.229	2.321
Si–C	1.933	1.916	1.925	1.932	–	1.924	1.933
Si–Si	2.364	2.381	2.386	2.372	–	2.370	2.363
Si–Li	2.481	2.504	2.488	2.490	–	2.478	2.481
Li–X	3.373	3.431	3.335	3.548	–	3.621	3.902
$\Sigma\alpha$	311.9	312.1	316.5	316.3	–	316.3	315.3
$\delta^{29}Si_{DFT}$	−110.9	60.6	23.8	−21.9	–	−24.0	−58.3
$\delta^{29}Si_{MP2}$	−113.5	76.4	38.2	−12.1	–	−30.5	−74.7
νSi–X	2099.6	724.5	731.6	735.5	–	432.6	450.0
E_{rel}	0.0	21.8	39.3	42.7	–	24.7	8.4
	4h	**4f**	**4o**	**4n**	**4cl**	**4s**	**4p**
Si–X	1.579	1.841	1.863	1.940	2.377	2.387	2.397
Si–C	2.015	1.993	1.980	1.993	1.989	1.991	2.005
Si–Si	2.414	2.454	2.453	2.432	2.432	2.434	2.410
Si–Li	2.482	2.564	2.584	2.562	2.681	2.667	2.576
Li–X	1.855	1.752	1.778	1.893	2.203	2.300	2.682
$\Sigma\alpha$	277.6	274.4	276.6	279.6	280.5	283.6	283.4
$\delta^{29}Si_{DFT}$	−134.9	52.0	28.8	−30.9	14.7	−50.0	−137.8
$\delta^{29}Si_{MP2}$	−145.6	68.3	19.6	−44.4	28.1	−59.2	−148.5
νSi–X	1746.9	471.0	512.4	511.4	264.1	320.0	329.3
E_{rel}	10.3	0.0	0.0	0.0	6.3	0.0	1.7

 © 2005 Wiley-VCH Verlag GmbH & Co. KGaA, Weinheim

distances in the crystals are in the range of 2.58 to 2.71 Å. The Si–Li bond lengths of the respective monomer units can be expected to be somewhat shorter. We find comparable bond lengths in our calculated structures. Furthermore, the investigated molecule set reveals that the more electronegative X is, the longer become the Si–Si bond lengths and the shorter are the Si–C bond lengths (see Table 2). In contrast to $H(H_3Si)MeSiLi$ and the $Me_n(H_3Si)_{3-n}SiLi$ molecules,[20,29,30] structure **1** is the most unstable of the four considered structure types in the gas phase, except for $X=PH_2$ (Tables 2 and 3).

Table 3. Selected bond lengths (Å), bond angle sum, δ^{29}Si, Si–X stretching frequency, and ZPVE-corrected relative energies (kJ mol^{-1}) for the silylenoid structures **2** and **3** of the $X(SiH_3)MeSiLi$ molecules.

	2h	**2f**	**2o**	**2n**	**2cl**	**2s**	**2p**
Si–X	–	1.847	1.850	1.910	2.392	2.410	2.397
Si–C	–	1.920	1.928	1.932	1.921	1.927	1.938
Si–Si	–	2.385	2.386	2.412	2.379	2.376	2.362
Si–Li	–	2.401	2.415	2.457	2.441	2.423	2.453
Li–X	–	1.756	1.773	1.945	2.238	2.370	2.482
$\Sigma\alpha$	–	302.9	306.0	306.4	302.1	302.7	310.1
$\delta^{29}Si_{DFT}$	–	152.1	79.6	31.3	125.2	32.4	−60.6
$\delta^{29}Si_{MP2}$	–	176.6	91.5	38.8	152.1	45.0	−58.1
νSi–X	–	443.8	503.9	486.3	242.8	325.0	320.5
E_{rel}	–	2.5	1.3	12.1	0.0	0.8	11.7
	3h	**3f**	**3o**	**3n**	**3cl**	**3s**	**3p**
Si–X	1.583	1.853	1.850	1.944	2.388	2.337	2.326
Si–C	1.925	1.922	1.928	1.932	1.917	1.923	1.926
Si–Si	2.385	2.442	2.386	2.378	2.406	2.393	2.383
Si–Li	2.318	2.551	2.415	2.394	2.479	2.457	2.468
Li–X	1.909	1.751	1.773	1.920	2.262	2.376	2.458
$\Sigma\alpha$	297.8	291.1	298.9	300.9	296.7	304.5	311.9
$\delta^{29}Si_{DFT}$	−97.2	144.7	79.0	11.1	107.5	−13.9	−74.9
$\delta^{29}Si_{MP2}$	−92.5	171.2	93.5	20.6	137.5	−2.0	−71.8
νSi–X	1738.7	439.5	490.1	490.8	226.5	302.4	429.9
E_{rel}	18.0	11.3	15.9	7.5	14.6	0.2	0.0

In the silylenoid structures **2** and **3**, as well as in the inverted structure **4**, the lithium cation interacts with X thus considerably elongating the Si–X bond (Table 3). While structure **2** does not exist for the $H(H_3Si)MeSiLi$ molecule, **2** forms the global minimum for the chlorosilyl anion in agreement with previous theoretical studies on simpler XH_2SiLi species.[3–6] Additional agostic interactions of Li^+ with the silyl group stabilize structure **3** making it the global minimum of $(H_2P)(H_3Si)MeSiLi$. The electrostatic interaction of the cation with all the substituents causes the inverted structure **4** to be the most stable gas-phase structure for the second-row substituents X = F, OH, NH_2, and for X = SH.

Despite the geometric changes and the presence of the Li cation, the δ^{29}Si chemical shifts of isomer **1** do not differ much from the bare silyl anion shifts. This can be explained by localized molecular orbital (LMO) analyses of the chemical shifts calculated by IGLO-DFT. While the formation of the Si–Li bond has a strong impact and deshields the silicon by 15–25 ppm, the contributions from the contraction of the Si–Si and Si–X single bonds are of similar size, but opposite sign. As a consequence, the net effect on the chemical shift is small. The increased silylenoid character of isomers **2** and **3** is reflected in the ^{29}Si chemical shifts by the downfield shift of up to 90 ppm. Interestingly, the δ^{29}Si of the inverted structures **4** resemble those of **1** in some cases making them indistinguishable by NMR measurements. This is surprising because there is no longer a direct interaction between the Si lone pair and Li in **4**. Furthermore, the Si–Si and Si–X bonds are significantly elongated. Again, LMO analyses reflect all these effects. As for isomer **1**, the shielding changes are of opposite sign, and the net effect on the chemical shift is small. The Si–X bond elongation in structures **2** and **3** is also reflected in the Si–X stretching frequencies that are between 219 and 285 cm^{-1} lower than in the tetrahedral structure **1**. These differences are much smaller for X = SH and PH_2.

As described for the free anions, the configuration inversion proceeds via a planar transition structure. All configuration inversion barriers are collected in Table 4. In agreement with previous results,[20] the least electronegative substituent, PH_2, has a comparatively low inversion barrier (ΔE_{inv} = 75.7 kJ mol^{-1}). For lithiated alkyl- and silyl-substituted silyl anions, the planar transition structure connects the tetrahedral (**1**) and the inverted (**4**) structures.[20] This also applies to the parent $H(H_3Si)MeSiLi$ molecule with an inversion barrier of 91.8/81.5 kJ mol^{-1}. In contrast, for our set of molecules, the inversion of the $X(H_3Si)MeSi$ framework occurs between structures **4**/**4′** and **3′**/**3**, with **3′** and **4′** being the respective enantiomers (Figure 3). In the transition structures, the cation resides between X and the SiH_3 group (similar to minimum **3**). Consequently, the Si–Si and Si–X bonds are slightly longer, and the Si–C bond is shorter than in the bare-anion transition structures. NBO analyses and Si–Si

Table 4. $X(SiH_3)MeSiLi$ energy barriers (kJ mol^{-1}) for configuration inversion and isomerization under configuration retention. The energy for the respective backreaction is given in parenthesis.

	Configuration inversion	Configuration retention		
X	**4→3′**	**4→2**	**2→3**	**2→1**
F	148.5 (137.2)	35.1 (32.2)	11.3 (2.5)	25.9 (6.7)
OH	132.6 (117.2)	43.5 (42.3)	16.3 (2.1)	37.7 (−23.0)
NH_2	118.4 (110.9)	28.9 (16.7)	1.7 (6.3)	37.7 (7.1)
Cl	133.9 (125.5)	32.6 (38.9)	15.1 (0.8)	–
SH	99.6 (99.6)	–	16.3 (15.5)	–
PH_2	75.7 (77.8)	–	–	3.8 (7.5)

© 2005 Wiley-VCH Verlag GmbH & Co. KGaA, Weinheim

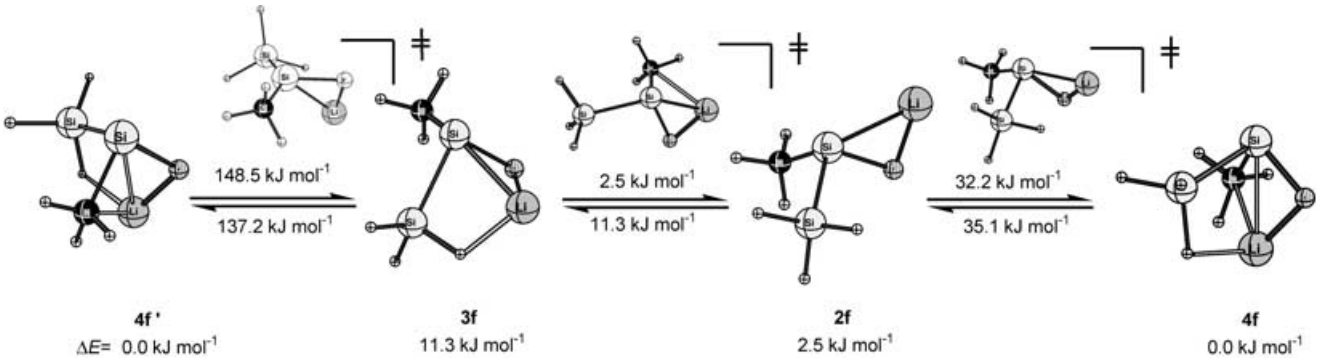

Figure 3. Enantiomerization of **4f/4f'** calculated at the B3LYP/6-31+G(d) level.

bond lengths again indicate the formation of a dative π bond between the central silicon and SiH_3. The energy barrier, now on average between 20–30 kJ mol^{-1} lower than for the bare anions, correlates with the electronegativity of X.

Isomerization from the inverted to the silylenoid structures **2** under configuration retention requires between 29–44 kJ mol^{-1} (Table 4). For X = SH and PH_2, the potential energy surface is very shallow with barriers below 15 kJ mol^{-1}. Although the Si–X bonds are elongated in the silylenoid and inverted structures, dissociation into the silylene $(H_3Si)MeSi$: and a LiX ion pair is unfavorable with the product energies lying between 115 and 255 kJ mol^{-1} above those of the reactants.

In apolar solvents, the $(R_3Si)_3SiLi$, $(R_3Si)_2MeSiLi$, and $(R_3Si)_2PhSiLi$ molecules[29,30] form cyclic dimers built from tetrahedral monomer units, the most stable calculated conformation in these cases.[20] We used $F(H_3Si)MeSiLi$ to investigate possible dimers built from **4f** and **2f** (Figure 4). Dimer **III**, built from two **4f** monomers, is 310 kJ mol^{-1} destabilized compared to the monomers. Both **II** and **I** are combinations of **2f** monomers. While **II** bears similarities to the dimer structures found in crystals from apolar solutions, **I**, the most stable of the three structures, can be regarded as the product of a selfcondensation, as described for the reaction in polar solutions.[9] Both dimers are more stable than the monomers; however, the formation energies involved are not known because we did not locate the respective transition structures (Table 5).

Addition of solvent molecules: In contrast to structures **3** and **4** with dipole moments below 4 debye, **1** and **2** have a dipole moment of ≈12 debye and will therefore be considerably stabilized by a polar solvent. Structure **1**·3dme, illustrated in Figure 5, is the most stable conformer for X = Cl, PH_2, SH, and NH_2. Owing to the solvent interaction, the Li–Si bond lengths are 2.63–2.64 Å, which is similar to the measured 2.68 Å of the amino-substituted compounds.[16,17] The Si–N bond length of 1.825 Å is also in the correct range (1.763–1.824 Å). In the silylenoid **2**·3dme, the cation only binds to X and has no direct interaction with the central Si atom. Only for $X = NH_2$, another minimum exists that is 3.7 kJ mol^{-1} more stable, in which the solvated Li^+ still interacts with both Si and N. The Si–X distances of **2**·3dme are shorter than in the gas-phase structures **2** where the Li–Si interaction is still present. Silylenoid structure **2**·3dme is the global minimum only for X = F and OH, in agreement with the crystal structure of $(Me_3Si)_2(MeO)SiK$.[14] Table 6 contains the most important bond lengths and relative energies for both structure types. **1**·3dme and **2**·3dme can easily interconvert with energy barriers below 15 kJ mol^{-1} (Table 5) and should both be present in solution at room temperature. Only **1p**·3dme is slightly more stable than

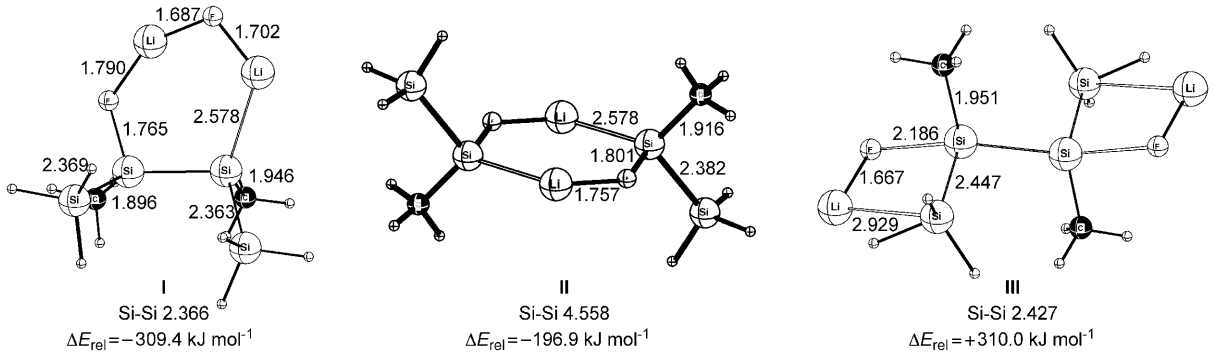

Figure 4. Gas-phase structures of $F(H_3Si)MeSiLi$ dimers.

 © 2005 Wiley-VCH Verlag GmbH & Co. KGaA, Weinheim

Table 5. Selected bond lengths (Å), bond angle sums, ZPVE-corrected relative energies (kJ mol^{-1}), and δ^{29}Si of the solvated XMe(H_3Si)SiLi molecules.

	1f	**1o**	**1n**	**1cl**	**1s**	**1p**
Si–X	1.728	1.772	1.825[a]	2.258	2.287	2.339
Si–C	1.934	1.943	1.949	1.935	1.942	1.949
Si–Si	2.400	2.402	2.386	2.384	2.383	2.372
Li–Si	2.628	2.625	2.630[a]	2.638	2.633	2.638
Li–X	3.250	3.223	3.639	3.614	3.993	3.964
$\Sigma\alpha$	302.5	305.8	306.2	300.0	299.8	306.0
δ^{29}Si	83.6	49.2	−15.4	47.6	−16.6	−82.3
E_{rel}	10.5	9.6	0.0	0.0	0.0	0.0
	2f	**2o**	**2n**	**2cl**	**2s**	**2p**
Si–X	1.826	1.839	1.919	2.393	2.397	2.350
Si–C	1.945	1.951	1.957	1.944	1.952	1.958
Si–Si	2.413	2.413	2.400	2.401	2.398	2.391
Li–Si	3.128	3.082	2.999	3.474	3.368	3.944
Li–X	1.805	1.859	2.023	2.326	2.466	2.548
$\Sigma\alpha$	290.0	293.0	293.1	288.9	289.0	294.1
δ^{29}Si	139.6	67.4	5.9	126.1	29.8	−75.9
E_{rel}	0.0	0.0	1.5	7.0	10.4	20.1

[a] Measured values for Li–Si are between 2.678[17] and 2.732 Å,[16] and values for N–Si are between 1.763 and 1.824 Å.

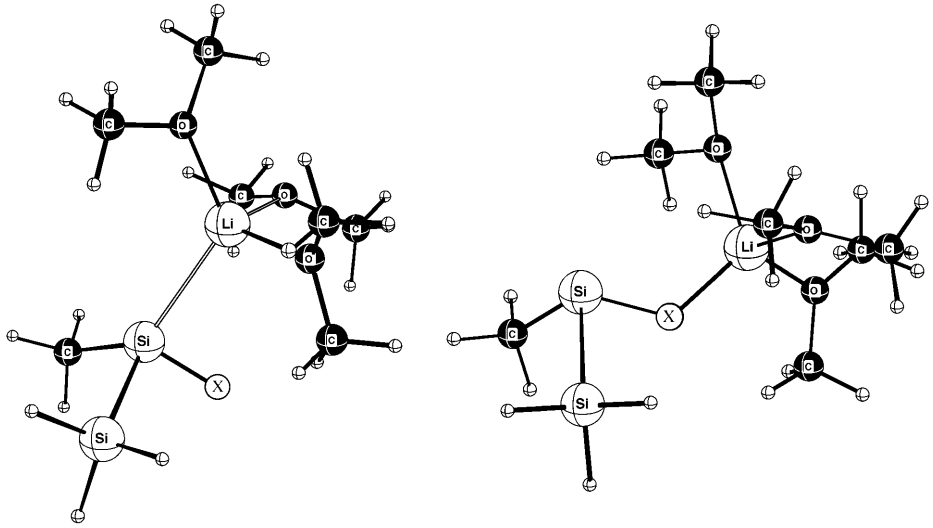

Figure 5. Tetrahedral (**1**·3 dme) and silylenoid (**2**·3 dme) structures of lithiosilanes with one electronegative substituent X = F, Cl, OH, SH, NH_2, and PH_2, in a polar solution.

Table 6. Isomerization and configuration inversion barriers (kJ mol^{-1}) of the solvated XMe(H_3Si)SiLi molecules.

X	$\Delta E_{\mathbf{1}\rightarrow\mathbf{2}}$ ($\Delta E_{\mathbf{2}\rightarrow\mathbf{1}}$)	$\Delta E_{\mathbf{1}\rightarrow\mathbf{2}}$	$\Delta E_{\mathbf{2}\rightarrow\mathbf{1}}$
F	169.7 (159.2)	3.4	13.9
OH	203.7 (213.6)	5.0	14.8
NH_2	143.9 (142.4)	12.3	10.8
Cl	160.2 (153.2)	10.8	3.0
SH	129.6 (130.2)	10.5	0.1
PH_2	113.8 (97.6)	26.2	6.2

2p·3 dme. As expected from the dipole moments, no solution structures corresponding to **3** and **4** could be located.

The chemical shifts of the solvated structures **1** are at most 25 ppm below their gas-phase values. In the silylenoid structures **2**·3 dme, δ^{29}Si value shifts downfield by 6–78 ppm. This effect is strongest for the halogenated lithiosilanes. Although measured δ^{29}Si data are available for amino-, alkoxy-, and thiolithiosilanes, a comparison is complicated by the differing substituent sizes and patterns. A detailed analysis of factors influencing heteroatom-substituted lithiosilanes has recently been performed for tetrahedral structures.[32] However, owing to the ease of interconversion, the tetrahedral as well as the silylenoid structures should be taken into account for a comparison with NMR measurements in solution.

In contrast to the gas phase, the configuration inversion with solvent molecules is energetically more demanding than for the bare anions (Table 6). From the transition structure, the solvated lithium cation rotates around the Si–X bond directly into minimum **2**·3 dme without formation of a **4**·3 dme intermediate (Figure 6). For those compounds with a tetrahedral structure as the global minimum (X = NH_2, Cl, SH, PH_2), the solvated cation resides on top of the silicon in the transition structure. For X = OH and F, the solvated lithium interacts both with X and Si (Figure 6). Owing to the relatively high energies involved, configuration-inversion reactions seem to be rather unlikely to occur.

The α elimination of XLi·3 dme becomes feasible in solution, especially for the halogenated lithiosilanes. The relative energies between reactants and products for X = F and Cl are $E_{rel} = -214.9$ and -280 kJ mol^{-1}. For X = SH, PH_2, OH, and NH_2, relative energies of 126.8, 173.8, 191.3, and 216.2 kJ mol^{-1} are found between reactants and products. However, to obtain the typical silylene-trapping reactions, the presence of a "free" silylene is not mandatory. Silylene–LiX adducts can react in the same way.[6,12,33] Starting from the **2**·3 dme minima, we increased the Si–X bond length stepwise. The energy profiles show a very shallow potential for **2cl**·3 dme and **2s**·3 dme (Figure 7). Loosening the Si–X bond by 0.6 Å takes less than 30 kJ mol^{-1}. The **2o**·3 dme and **2f**·3 dme are not prone to silylene reactions. Confirmation

© 2005 Wiley-VCH Verlag GmbH & Co. KGaA, Weinheim

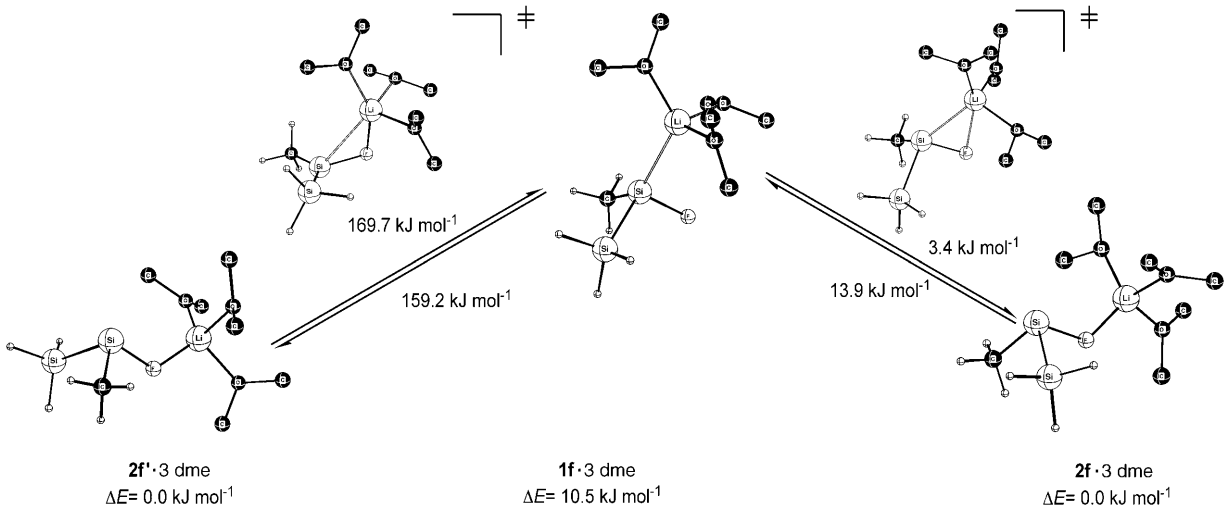

Figure 6. Configuration inversion and retention reaction for a solvated lithiofluorosilane.

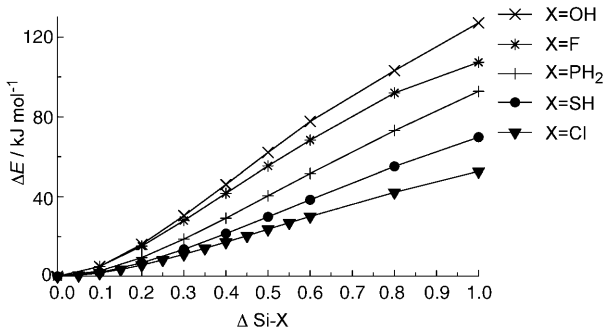

Figure 7. Energy profiles for the Si–X bond elongation in the silylenoid structures **2**·3 dme.

comes from the selfcondensation reaction of fluorosilanes,[9] in contrast to the reaction of chlorosilanes with *t*BuOK that leads to complex product distributions.[9] In a recent study of lithiated thiosilanes, these compounds are described as "α-eliminative silylenoids readily releasing the corresponding silylenes".[19] The profile of the amino-substituted lithiosilane looks quite irregular owing to the Li–Si interaction in **2n**·3 dme. At 0.05 Å, the energy increases by more than 55 kJ mol^{-1} as the Si–Li interaction disrupts. Once this barrier is overcome, the curve is between those of fluoro- and phosphinolithiosilane.

Dimerization reactions have not been investigated for the solvated lithiosilanes owing to the molecule sizes and the associated computational demands.

Conclusion

Silyl anions with one electronegative substituent are configurationally stable. For the bare anions X(SiH$_3$)MeSi with X = F, OH, NH$_2$, Cl, SH, and PH$_2$, configuration inversion demands energies between 107 and 167 kJ mol^{-1}. Adding a lithium counterion gives rise to four different low-energy structures. In the gas phase, the inverted structure is extremely stable owing to the electrostatic stabilization of the Li cation. The silylenoid structures are close in energy (up to 7.5 kJ mol^{-1}) and the isomerization barriers are low (< 9 kJ mol^{-1}). The molecules with X = Cl and PH$_2$ are exceptions because the silylenoid is the most stable structure. The classical tetrahedral structure is unfavorable for all of the considered X substituents in the gas phase (ΔE_{rel} > 20 kJ mol^{-1}). The presence of the lithium cation lowers the configuration inversion barrier by approximately 30 kJ mol^{-1}. The α elimination of LiX is not favorable and is unlikely to occur as an alternative to the configuration inversion in the gas phase.

In polar solutions, only the tetrahedral and the silylenoid structure are minima. The tetrahedral structure is preferred by all species apart from X = F and OH. Isomerization to the silylenoid structure requires energies of less than 15 kJ mol^{-1}, which indicates an increased reactivity. Configuration inversion in X(H$_3$Si)MeSiLi·3 dme molecules requires higher energies than those in the gas phase and is not likely to occur. For the halogenated species, especially for X = Cl, the decomposition into a silylene and a LiX moiety results in an energy gain. However, to react as silylene it is sufficient to loosen the Si–X bond to simultaneously form a silylene–LiX adduct. Especially for the thio- and chlorolithiosilanes, this is likely to occur.

Acknowledgements

The authors thank the Austrian Fonds zur Förderung der wissenschaftlichen Forschung for continuous financial support (projects T-101 and Y-120).

[1] A. C. Hopkinson, M. H. Lien, *Tetrahedron* **1981**, *37*, 1105.
[2] K. Tamao, A. Kawachi, M. Asahara, A. Toshimitsu, *Pure Appl. Chem.* **1999**, *71*, 393.
[3] T. Clark, P. von R. Schleyer, *J. Organomet. Chem.* **1980**, *191*, 347.

 © 2005 Wiley-VCH Verlag GmbH & Co. KGaA, Weinheim

[4] S. Feng, D. Feng, *J. Mol. Struct.* **2001**, *541*, 171.
[5] S. Feng, D. Feng, C. Deng, *Chem. Phys. Lett.* **1993**, *214*, 97.
[6] Y. Tanaka, M. Hada, A. Kawachi, K. Tamao, H. Nakatsuji, *Organometallics* **1998**, *17*, 4573.
[7] P. C. Gomez, M. Alcolea Palafox, L. F. Pacios, *J. Phys. Chem. A* **1999**, *103*, 8537.
[8] L. F. Pacios, O. Galvez, P. C. Gomez, *J. Phys. Chem. A* **2000**, *104*, 7617.
[9] R. Fischer, J. Baumgartner, G. Kickelbick, C. Marschner, *J. Am. Chem. Soc.* **2003**, *125*, 3414.
[10] M. Flock, A. Dransfeld, *Chem. Eur. J.* **2003**, *9*, 3320.
[11] M. E. Lee, H. M. Cho, M. S. Ryu, C. H. Kim, W. Ando, *J. Am. Chem. Soc.* **2001**, *123*, 7732.
[12] M. E. Lee, H. M. Cho, Y. M. Lim, J. K. Choi, C. H. Park, S. E. Jeong, U. Lee, *Chem. Eur. J.* **2004**, *10*, 377.
[13] K. Tamao, A. Kawachi, *Angew. Chem.* **1995**, *107*, 886; *Angew. Chem. Int. Ed. Engl.* **1995**, *34*, 818.
[14] R. Likhar, M. Zirngast, J. Baumgartner, C. Marschner, *Chem. Commun.* **2004**, 1764.
[15] K. Tamao, A. Kawachi, *J. Am. Chem. Soc.* **1992**, *114*, 3989.
[16] A. Kawachi, K. Tamao, *J. Am. Chem. Soc.* **2000**, *122*, 1919.
[17] C. Strohmann, O. Ulbrich, D. Auer, *Eur. J. Inorg. Chem.* **2001**, 1013.
[18] A. Kawachi, H. Maeda, K. Tamao, *Organometallics* **2002**, *21*, 1319.
[19] A. Kawachi, Y. Oishi, T. Kataoka, K. Tamao, *Organometallics* **2004**, *23*, 2949.
[20] M. Flock, C. Marschner, *Chem. Eur. J.* **2002**, *8*, 1024.
[21] Gaussian 98 (Revision A.7), M. J. Frisch, G. W. Trucks, H. B. Schlegel, G. E. Scuseria, M. A. Robb, J. R. Cheeseman, V. G. Zakrzewski, J. A. Montgomery, Jr., R. E. Stratmann, J. C. Burant, S. Dapprich, J. M. Millam, A. D. Daniels, K. N. Kudin, M. C. Strain, O. Farkas, J. Tomasi, V. Barone, M. Cossi, R. Cammi, B. Mennucci, C. Pomelli, C. Adamo, S. Clifford, J. Ochterski, G. A. Petersson, P. Y. Ayala, Q. Cui, K. Morokuma, D. K. Malick, A. D. Rabuck, K. Raghavachari, J. B. Foresman, J. Cioslowski, J. V. Ortiz, B. B. Stefanov, G. Liu, A. Liashenko, P. Piskorz, I. Komaromi, R. Gomperts, R. L. Martin, D. J. Fox, T. Keith, M. A. Al-Laham, C. Y. Peng, A. Nanayakkara, C. Gonzalez, M. Challacombe, P. M. W. Gill, B. G. Johnson, W. Chen, M. W. Wong, J. L. Andres, M. Head-Gordon, E. S. Replogle, J. A. Pople, Gaussian, Inc., Pittsburgh, PA, **1998**.
[22] V. G. Malkin, O. L. Malkina, L. A. Eriksson, D. R. Salahub in *Theoretical and Computational Chemistry*, *Vol. 2* (Eds.: J. M. Seminario, P. Politzer), Elsevier, Amsterdam, **1995**, 273.
[23] J. P. Perdew, Y. Wang, *Phys. Rev. B* **1992**, *169*, 387.
[24] a) A. St-Amant, D. R. Salahub, *Chem. Phys. Lett.* **1990**, *169*, 387; b) D. R. Salahub, R. Fournier, P. Mlynarski, I. Papai, A. St-Amant, J. Ushio in *Density Functional Methods in Chemistry* (Eds.: J. Labanowski, J. Andzelm), Springer, New York, **1991**.
[25] W. Kutzelnigg, U. Fleischer, M. Schindler, NMR *Basic Principles and Progress*, *Vol. 23*, Springer, Berlin, **1990**.
[26] A. L. Allred, E. G. Rochow, *J. Inorg. Nucl. Chem.* **1958**, *5*, 264.
[27] M. S. Gordon, D. E. Volk, D. R. Gano, *J. Am. Chem. Soc.* **1989**, *111*, 9273.
[28] J. R. Damewood, C. M. Haddad, *J. Phys. Chem.* **1988**, *92*, 33.
[29] K. W. Klinkhammer, *Chem. Eur. J.* **1997**, *3*, 1418.
[30] Y. Apeloig, M. Yuzefovich, M. Bendikov, D. Bravo-Zhivotovskii, D. Bläser, R. Boese, *Angew. Chem.* **2001**, *113*, 3106; *Angew. Chem. Int. Ed.* **2001**, *40*, 180.
[31] M. Nanjo, A. Sekiguchi, H. Sakurai, *Bull. Chem. Soc. Jpn.* **1999**, *72*, 1387.
[32] D. Auer, M. Kaupp, C. Strohmann, *Organometallics* **2004**, *23*, 3647.
[33] N. Wiberg, W. Niedermayer, G. Fischer, H. Nöth, M. Suter, *Eur. J. Inorg. Chem.* **2002**, 1066.

Received: December 31, 2004
Published online: June 15, 2005

© 2005 Wiley-VCH Verlag GmbH & Co. KGaA, Weinheim